Proceedings of Montreal 2018
Global Power and Propulsion Forum
7th – 9th May, 2018
www.pps.global

GPPS-NA-2018-119

EQUATION OF STATE COMPARISONS AND EVALUATIONS FOR APPLICATIONS THROUGH GAS PROPERTY TESTING AND DERIVATIONS

Sarah B. Simons
Southwest Research Institute
sarah.simons@swri.org
San Antonio, Texas, USA

Brandon L. Ridens
Southwest Research Institute
brandon.ridens@swri.org
San Antonio, Texas, USA

Shane B. Coogan
Southwest Research Institute
shane.coogan@swri.org
San Antonio, Texas, USA

Dr. Rainer Kurz
Solar Turbines, Inc.
Kurz_Rainer_X@solarturbines.com
San Diego, California, USA

Dr. Klaus Brun
Southwest Research Institute
klaus.brun@swri.org
San Antonio, Texas, USA

ABSTRACT

Accurate gas property prediction is a necessary component throughout the oil and gas industry for end users, operators and equipment manufacturers for proper sizing and selection of equipment, improving overall efficiency, and reducing operating costs. Various Equation of State (EOS) models are utilized to predict thermophysical gas properties needed for such calculations. These are semi-empirical models that allow the calculation of thermodynamic and dynamic properties such as density, enthalpy, and entropy of gas mixtures for known pressures and temperature (and vice versa). While there is a large body of work available comparing the results of various EOS models, there is currently limited or no data publically available to verify the results of these EOS calculations for the range of pressures, temperatures and gas compositions relevant to compression and pipeline operations [1-5]. This is specifically true for natural gas compositions containing heavier hydrocarbons, sour or acid gas components or high CO_2 content as well as operating points near the critical phase, high pressures, or dense phase (supercritical) operation. Thus, the users of EOS (operators and manufacturers) often have no precise data to determine whether a particular EOS will give sufficiently accurate results or which EOS will provide calculations closest to measured values.

In order to have an improved understanding of the applicability of standard EOS in pipeline applications, a set of gas physical property tests were undertaken with sweet and sour natural gas and CO_2 mixtures at typical pipeline compositions and conditions, including new high pressure dense phase applications. Specific gas properties tested include gas density (ρ), specific heat at constant volume (c_v), and speed of sound (c or SOS). These results were compared to several of the most commonly used EOS, including NIST, GERG, AGA8, PR, and SRK, which were also compared to each other.

This project was a joint effort with funding and direction from the Gas Machinery Research Council (GMRC) and the Pipeline Research Council International (PRCI).. A committee formed by representatives from GMRC, PRCI and the Southwest Research Institute® (SwRI®) defined the gas mixtures and test points presented in this paper. Table 1 and Table 2 provide the gas mixture component concentrations (in % mol) for the GMRC and PRCI portions of the project, respectively.

The purpose of this project is not to provide a comprehensive database, but rather provide data sets for multi-component gas mixtures, at pressures and temperatures relevant to gas compression and pipeline metering applications. While a large body of test data exists for pure substances and binary mixtures, data on gas compositions typical for many upstream and midstream oil and gas projects is very rare. Typical gas mixtures contain methane and heavier hydrocarbons, but may also include CO_2, nitrogen and water. The data sets obtained in this project can be used to test EOS model predictions against.

Also included in the scope of work for this project is the methodology for calculating enthalpy and entropy from experimental data. These properties cannot be measured and must be derived by their relationship to measured properties. Analyses performed for compressor performance, station operation, pipeline simulation all depend on these properties. Therefore, deriving equations that allow enthalpy and entropy

to be calculated from the tested properties is vital. The methodology for deriving these equations, as well as, the equations themselves are also presented.

TEST DESCRIPTION

The project committee defined the temperature and pressure test points to be used during the measurement campaign in an effort to represent conditions typically encountered with the defined mixtures and processes they are used with. The test runs were performed over the course of an 18-month period. Primary testing was completed first for each test mixture, followed by targeted repeat runs to reduce test uncertainty. The test matrices for the seven (7) mixtures and the desired temperature and pressure condition are shown in Table 1 through Table 4.

The test uncertainties are calculated for the primary direct measurements and reference condition at each test condition. The direct measurement uncertainty is a function of the sensor or equipment measurement uncertainty (i.e., scale or microphone precision) and additional uncertainties in the test geometry (i.e., length or internal volume) that directly affect the measured property. The instrument uncertainties, referenced as condition uncertainty, are uncertainties associated with the state point conditions (pressure, temperature, EOS model prediction, and gas mixture uncertainty) that are used as references when comparing the measurement to EOS. The reference uncertainty is highly dependent on the EOS used and varies with gas composition.

The reference condition uncertainty varied from 0.1% to 2.5% depending on the test condition. The driving factor for the larger uncertainties in the reference condition is typically attributed to either the temperature or mixture component uncertainties depending on the specific mixture and test point (their sensitivity in influencing the predicted property from the EOS)

Based on the range of test pressures in the Industry Project test program and the accuracy requirements, three (3) test fixtures were required as follows:

1. High Pressure/Concentrated Volume (for precision scale measurements of density at high pressures): This cylinder is rated for 1,380 bar and comprises an internal diameter of 51 mm with 0.15 m in length, accompanied by two pressure taps for a 1/4″ NPT thredolet connection to accommodate the high accuracy RTD, pressure transducer and fill line. The autoclave is placed vertically on the scale to take the mass measurements.
2. High Pressure/Concentrated Volume (for specific heat testing): This cylinder utilizes a similar design such as the autoclave used for the density testing, rated for 1,380 bar and comprises an internal diameter of 51 mm with 0.15m in length. A larger high pressure tap is incorporated to accommodate a heating element. An additional pressure tap is available for the RTD, pressure transducer and fill line.
3. High Pressure Fixture (for all SOS testing): Composed of high pressure assembled tubing rated for 690 bar, the test fixture is 14 mm diameter and approximately 1.2 m chamber length. By design, to determine the resonant frequency, there are five (5) high-pressure fittings along the fixture's length for dynamic pressure (using an internal microphone), static pressure, temperature, and fill-line purposes. One spare test port exists as a back-up for sensor access.

EOS COMPARISON

To compare the experimental test data with EOS model predictions, measured temperature and pressure conditions were used to predict the density, SOS, and specific heat at constant volume values according to the GERG-2008, NIST, AGA8, Peng-Robinson (P-R), and SRK EOS models. Modeling for GERG, NIST, AGA8, and P-R was performed using NIST REFPROP software version 9.1 and SRK with the Peneloux modification using the Calsep PVT SIM Nova software version 1.2, which provide EOS model outputs.

Although some variation in test results is noted due to the test uncertainty, significantly around the critical point, there are specific trends which are notable for the mixtures and particular test conditions. The following observations can be made regarding use of the various EOS models for mixtures analyzed in this test campaign.

EOS SOFTWARE IMPLEMENTATION

In other related work, it was found that for a particular EOS, implementation of the mixing laws and associated calculations can vary significantly depending on the software used. One particular EOS, RK/SRK, was evaluated for a typical heavy natural gas consisting of 46.5% Methane, 8% Ethane, 5% Propane, 3% I-Butane, 0.5% I-Pentane, 24% Nitrogen, and 5% Carbon Dioxide (all by Mol weight %) at fixed conditions. The results of the predictions are in the data shown in Table 5.

As shown in Table 5, various implementations of the same EOS, at the same test condition will give differing results. Specifically, for this gas composition and operating point chosen by the committee, the implementation of SRK was compared between PVT Sim, Multi-flash, REFPROP, SwRI's internal implementation software and an OEM's internal implementation software. Significant differences in results were found. The software used in implementing an EOS should also be taken into consideration.

DENSITY

The GMRC section of this project covered a wide range of components including a high CO_2 mixture, high CH_4 mixture, a complex blend of CO_2 and CH_4, and an acid gas mixture with H_2S. While each mixture provided individual trends with EOS results, there are common results that span most of the mixtures. When comparing the EOS model results to each other, the difference between the SRK and P-R EOS to the other EOS increases as pressure increases for all

temperature ranges of the GMRC mixtures. The PRCI mixtures, those containing larger amounts of heavy hydrocarbons, follow the same trend at elevated temperatures but have relatively unchanging and significant differences between SRK and P-R EOS to the other EOS over the entire pressure range reviewed at temperatures near the critical temperature. Figure 1 demonstrates this trend by displaying the percent difference of the EOS model results for the specific state points and the experimental data over the pressure range measured.

Overall, the GERG, NIST and AGA8 EOS provide very similar results of density for most of the mixtures and state points in this project. Exceptions occur with the elevated pressure and temperature operating points with the GMRC Mix 3, the acid gas mixture, seen in Figure 2. Similar trends are present at lower temperatures and higher pressures with PRCI Mix 2 and Mix 3. Figure 3 demonstrates the density difference between the three (3) EOS with the AGA8 EOS predicting approximately 1% higher density values than GERG and NIST. This trend of AGA8 providing higher values of density than GERG and NIST is seen for all of the mixtures in this project. It can be inferred that the increased presence of heavier hydrocarbons in the mixtures lead to the AGA8 EOS providing relatively higher values of density than GERG and NIST.

For the majority of the mixtures measured in this project, the GERG, NIST, and AGA8 EOS match the experimental density data within +/- 1%. The highest deviation from the experimental data for GERG, NIST and AGA8 with the GMRC mixtures occurred with Mix 1 at temperatures above 200°F and Mix 3 at temperatures above 300°F, under predicting values by approximately 1.5% to 2%. For the acid gas GMRC Mix 3, the GERG, NIST, and AGA8 EOS match the experimental density values under 0.5% for the pressure points at 120°F while under predicting by approximately 0.5% and increasing to -1.5% as pressure rises, as seen in Figure 2. The GERG, NIST, and AGA8 EOS provided the best correlation with experimental data with GMRC Mix 4, slightly under predicting density values by less than 1% for all pressure and temperature state points reviewed.

The P-R and SRK EOS provide the largest deviation from the density measurements in the project. The SRK EOS under predicts density for all of the mixtures and test points by roughly 2% to 4% at elevated pressures. For the GMRC mixtures, the SRK EOS finds better correlation to both the other EOS models and the experimental data at the lowest pressure and temperature points, as demonstrated in Figure 4. The SRK EOS for the PRCI mixtures, however, deviate at least roughly 1.5% for all state points reviewed. The concentration of the heavy hydrocarbons in the PRCI mixtures lead to higher deviations in density for the SRK EOS throughout the entire pressure and temperature range reviewed. The close proximity to the critical point of CO2 in GMRC Mix 1, causes the highest deviation for both the P-R and SRK EOS, reaching a maximum deviation from the experimental values by approximately -9% and -15%, respectively as seen in Figure 4. Below the critical point, the all of the EOS match more closely to each other within approximately +/- 1% of the measured density value.

The P-R EOS did not follow the same trends as the other EOS reviewed. For the majority of reviewed PRCI mixtures, P-R typically followed similar trends as the SRK EOS with slightly smaller deviations, as seen in Figure 1 and Figure 3. However, there are many mixtures in which the P-R EOS matches the experimental data and other EOS well at lower pressures and deviates linearly as pressure increases, as seen in Figure 5. This trend is typically apparent with isotherms at elevated temperatures. While the P-R EOS tends to provide lower values of density than the GERG, NIST, and AGA8 EOS for the majority of mixtures and state points, there are instances when the P-R EOS provides higher values. Figure 2 and Figure 4 demonstrate this occurrence which arises with all of the GMRC mixtures at lower pressures (below 2000 psi) and PRCI Mix 1 and 2 at elevated temperatures (above 150°F) and lower pressures (below 2000 psi), as seen in Figure 6.

SOS

Similar differences in SOS measured results versus predicted results were found when comparing SRK and P-R calculations to the other three (3) EOS (GERG, NIST, and AGA8). As with the density results, the largest difference between the EOS models is seen with GMRC Mix 1, the mixture with the highest CO_2 content. Figure 7 shows a difference of approximately 20% near the critical point between the EOS when comparing SRK to AGA8 with approximately 15% deviation from the measured results for the P-R EOS. The second largest deviation between the EOS for the GMRC mixtures is Mix 2, containing roughly 45% mol CO_2, with the SRK and P-R EOS deviating approximately 5% from the other EOS, as seen in Figure 8. The largest deviations between EOS results throughout the project scope are present at test points in proximity to the mixture's critical point.

The largest deviations between the EOS SOS results found with the PRCI mixtures are approximately 10% for both PRCI Mix 2 and 3, demonstrated in Figure 9. SOS results from P-R and SRK generally decrease linearly as pressure increases for most isotherm ranges. Exceptions to this downward trend are present in the 212°F isotherm ranges for PRCI Mix 2 and 3 and demonstrated in Figure 10. For most state conditions, P-R and SRK predict higher values of SOS than GERG, NIST and AGA8. For conditions when the downward trend is present for P-R and SRK, there is a state at which the two (2) EOS begin to provide lower values of SOS, as seen in Figure 9. This transition is present for the 32°F isotherm for PRCI Mix 1 and 2 and increases with the heavy hydrocarbon content for the 77°F and 122°F isotherms for PRCI Mix 3. Similar trends are not as apparent with the GMRC mixtures. The P-R and SRK EOS typically providing higher values of SOS than the remaining EOS for the GMRC mixtures at lower pressures (below 2000 psi) and slightly higher values at higher pressures (above 2000 psi), excluding GMRC Mix 4.

The GERG, NIST, and AGA8 EOS match well with each other and deviate within +/- 2% from the measured values of SOS for the majority of GMRC Mix 1 results. As seen in Figure 7, deviations near the critical point of the mixture reach approximately -5% for the three (3) EOS, with higher deviations observed with P-R and SRK. Results are more varied with GMRC Mix 2, the blend of primarily CO_2 and CH_4, with GERG, NIST, and AGA8 over predicting by approximately 1% at lower pressures at the 100°F state points and under predicting by approximately 2% at elevated pressures (1500 psia), seen in Figure 8. As the temperature rises with GMRC Mix 2, the three EOS over predict SOS values by approximately 2% compared to the measured values for the 1500 psia ranges and rises to approximately 3.5% difference for the 3500 psia ranges, seen in Figure 11. However, the AGA8 EOS provides notably lower SOS values than the other EOS results by approximately 1% for state conditions reviewed above 300°F for GMRC Mix 2. Similar trends for AGA8 are present for the 3500 psia state conditions above 250°F for GMRC Mix 3, shown in Figure 12.

Lower deviations in SOS results are seen in GMRC Mix 3 than in Mix 1 and 2. For the 120°F state conditions, the average deviation is approximately -1.25% for GMRC Mix 3. At higher temperatures, those above 250°F, deviations in calculated SOS from the measured values were under 0.5% for the GERG, NIST, AGA8, and P-R. Figure 12 shows the under prediction in SOS for all of the EOS for GMRC Mix 3 from approximately -1.5% to -2.5% as the pressure rises to 3500 psia. The GMRC Mix 4 had the lowest deviations in SOS calculations overall for the entire project. For this primarily methane mixture, the GERG, NIST, and AGA8 EOS under predict the SOS values by approximately 1% for pressures at 100°F and under 0.5% for temperatures above 250°F.

Similar to the GMRC mixtures, the GERG, NIST, and AGA8 EOS match well with each other and deviate within +/- 2% from the measured values of SOS for the majority of PRCI results. Particularly, the three (3) EOS models over predict SOS from 0.1% to 2% for the 32°F state points for PRCI Mix 1. The EOS models under predict the SOS values compared to the experimental measurements for higher temperatures, -0.5% to -2% decreasing with rising pressure for both the 122°F and 212°F ranges, as seen in Figure 13. Deviation trends are more extreme for PRCI Mix 2 with the GERG, NIST, and AGA8 EOS over predicting SOS values by 1% to 2.5% in the 32°F range. Deviations are larger with the 122°F range, under predicting SOS values for PRCI Mix 2 by 1% to 3%, as seen in Figure 14. The lowest deviations are present at the highest temperature range for PRCI Mix 2, 212°F, with the deviation ranging from 0.5% to -1%. PRCI Mix 3, with its increased heavy hydrocarbon content, had the largest range of deviation from the experimental data of the three (3) mixtures. The GMRC, NIST, and AGA8 EOS deviated from the measurements by approximately 2.5% to -1.5% for the 77°F range, decreasing in value as pressure increases seen in Figure 15. The EOS models under predict SOS values for PRCI Mix 3 by approximately 0.5% to 2% for the 122°F range. In a reverse trend of the 77°F range, deviations from the measured value range from approximately -1% to 2% for the 212°F range, with a positive slope as pressure increases for PRCI Mix 3.

SPECIFIC HEAT AT CONSTANT VOLUME

In general, there are higher deviations in the EOS predictions of specific heat at constant volume than there are for density and SOS in the mixtures evaluated for this project. Similar to the other properties, P-R and SRK deviate significantly from GERG, NIST, and AGA8. The highest deviation between the EOS is present near the critical points of GMRC Mix 1 and PRCI Mix 3, seen in Figure 16 and Figure 17 respectively. The largest difference between P-R and SRK with the other EOS for the GMRC mixtures is approximately 15%, providing significantly lower values of c_v. The largest scatter in calculated c_v from the EOS is in the PRCI mixtures, with AGA8 deviating from GERG and NIST to create a difference of 15% between the AGA8 and P-R EOS near the critical point of PRCI Mix 3. Based on the model results of the mixtures and state points reviewed in this paper, the more complex c_v calculations from EOS models are significantly more sensitive near the critical point than with density and SOS. For the GMRC mixtures, the EOS have good correlation with each other at the lowest pressure and temperature state points as seen in Figure 18. For the majority of conditions tested, the SRK EOS over predicts c_v values than the remaining EOS with exceptions for GMRC Mix 1 and 2 and all of the PRCI mixtures at low temperatures, exemplified in Figure 16 and Figure 17.

Specific heat at constant volume has the largest deviation overall of the physical properties measured in this project. The largest deviations that the EOS have from the measured c_v for the GMRC mixtures is near the critical point of GMRC Mix 1, as seen in Figure 16. At this test point, GERG, NIST and AGA8 under predict c_v by approximately 10% while SRK and P-R under predict by a range of approximately 20% to 25%, respectively. At lower temperatures, the EOS have a deviation of approximately -5% for GMRC Mix 1. As pressures increase above the critical point of this CO_2 mixture, the EOS over predict c_v by approximately 1.5% with a larger scatter between the EOS models. The introduction of methane into the mixture increases the overall offset of the EOS predictions while still remaining under those seen near the critical point. A relatively wide range of deviation is present with the 100°F isotherm of GMRC Mix 2, having a different ranging from 2% to 8% between the EOS model predictions and experimental data, increasing with pressure near the critical point, as seen in Figure 19. As temperatures rise to around 200°F, the GERG, NIST, AGA8, and P-R EOS over predict c_v approximately 1% to 3% for PRCI Mix 2. Deviations of these EOS increase to approximately 4.5% to 5% for state points above 300°F. Unlike the other mixtures, the P-R EOS had the lowest deviations from the GMRC Mix 2, matching the experimental data the closest among the EOS reviewed.

EOS predictions of c_v for the GMRC Mix 3 had lower deviations from the experimental data. The EOS under predicted values of c_v for this mixture by approximately 2% with higher scatter between the models at 1500 psia for the 120°F isotherm, as seen in Figure 16. Deviations increased to approximately -4% for temperatures above 250°F. For the GMRC Mix 3, the AGA8 EOS matched the experimental measurements the best for the data set presented in this paper.

As with the density and SOS results, the lowest deviations seen in the examined mixtures are with GMRC Mix 4, the highly concentrated methane hydrocarbon mixture. For the 100°F state points, the EOS models match the experimental data within 1%, excluding P-R at 1500 psia, as seen in Figure 20. At temperatures above 250°F, the GERG, NIST, and AGA8 EOS over predict c_v values for GMRC Mix 4 by approximately 1.5% compared to experimental measurements. The SRK EOS over predicted c_v values by approximately 4% to 6% over the pressure range.

EOS model deviations are significantly higher for the PRCI mixtures. The concentration of heavier hydrocarbons lead to lower phase boundary conditions for the three (3) mixtures and the measured state points are closer to the critical point of the mixtures. The PRCI Mix 1 had the lowest deviations of the three (3) mixtures, with the GERG, NIST, and AGA8 EOS models over predicting c_v values by approximately 5.5% to 11% for the 32°F state conditions, increasing with pressure as seen in Figure 21. Deviations from the measured data decrease as temperature increases, ranging from approximately 4.5% to 5% for the 122°F isotherm and approximately 2.5% to 5.5% for the 212°F isotherm of PRCI Mix 1.

Deviations in EOS model predictions increase as the heavier hydrocarbon concentrations in the mix rises. Based on the measurement results, the GERG and NIST EOS over predict c_v values of PRCI Mix 2 by approximately 17% for the 32°F conditions. As shown in Figure 22, AGA8 provides lower values of c_v in this range and decreases significantly as pressure rises. The opposite trend is seen with the P-R and SRK EOS, where their values rise as pressure rises in this isotherm, matching the GERG and NIST results better at higher pressures. The GERG and NIST EOS over predict c_v values by approximately 12% to 15% for the 122°F data set, decreasing in pressure, as seen in Figure 22. For this range, the P-R EOS matches the experimental data more favorably, over predicting by approximately 7% to 12%. The lowest deviations for GMRC Mix 2 are seen at the highest temperature conditions, 212°F. Unlike the other temperature isotherms, the EOS model predictions do not follow an apparent fall or rise due to the pressure gradient. Across the pressure range, the GERG and NIST EOS deviated from the experimental data by approximately 7% to 8%. Similar to the 122°F isotherm, the P-R EOS provided the lowest deviation across the 212°F state conditions.

The largest deviations seen in this project are associated with the c_v EOS predictions of PRCI Mix 3. As stated above, the lowest temperature points were raised from 32°F to 77°F to avoid the saturated liquid phase due to the elevated concentration of heavy hydrocarbons in the mixture. Because the two-phase envelope of the mixture extends past room temperature, as seen in Figure 23, and the mixture could only be stored at pressures below the two-phase boundary to maintain a homogenous mixture, the PRCI Mix 3 was stored at pressure of approximately 325 psia while at a room temperature of 75°F. To pressurize the test cylinders from this initial state point, the mixture would unavoidably cross through the two-phase region throughout the system. Demonstrated in Figure 23, this would occur with possibly all of the measurement conditions, primarily those at temperature of 77°F and 122°F. While the mixture is in the two-phase region, heavier hydrocarbons drop out (liquefy) and the mixture is no longer in a homogenous state, stratifying when pressurized into the test fixtures. Even when pressurized and heated to a superheated vapor, there are no certain means of remixing the steady state mixture to reinstate homogeneity. The c_v measurements are more sensitive to this stratification of the mixture than density and SOS. Calculations of experimental c_v assume even distribution of the mixture within the autoclave when the gas is heated by a single source near the center of the test fixture. If the mixture is stratified, uneven heating of the gas will occur leading to higher deviations in c_v results. Because of this, significantly higher deviations are expected in the test measurements compared to what may occur in the field when the mixture remains in a homogenous state.

As stated before, PRCI Mix 3 has notably higher deviations than the other mixtures reviewed in this project, over predicting by approximately 30% to 47% 77°F state points, decreasing significantly as pressure increases as seen in Figure 17. As isotherm temperatures rise to 122°F, overall deviations of the GERG and NIST EOS model predictions from the measured c_v decrease to approximately 27% to 33%. At the same state points, P-R over predicted c_v values of PRCI Mix 3 by approximately 20% to 28%. Deviations were even lower for the 212°F isotherm, with the GERG, NIST, AGA8 and SRK EOS over predicting by approximately 13% to 18%. Similar to the lower temperature points, the P-R EOS provided the lowest deviation for this data set, over predicting by approximately 12.5% to 15% as seen in Figure 24.

COMPARISON OF EOS FOR PRCI MIXTURES NEAR THE CRITICAL POINT

Since the goal of the PRCI mixture tests is to evaluate predictions near the phase line, the EOS calculations were graphed against the measured pressure in relation to the critical pressure for each temperature. This also allowed the EOS predictions for each mixture over the entire operating range to be shown on one graph for comparison purposes. PRCI Mix #2 results are shown in Figure 25 through Figure 27 below. Higher temperatures, further away from the critical

temperature, on average provided more accurate predictions when testing near the critical pressure.

Enthalpy and Entropy Derivations

The basic properties of pressure, temperature, and specific volume (or density) are fundamentally defined by how they are measured and can be directly observed by experiment. Other quantities involving the derivatives of thermodynamic properties can also be measured, such as the SOS and the specific heat at constant volume. Conversely, enthalpy and entropy, while just as fundamental as the basic properties, are derived quantities that cannot be directly measured. These crucial properties must be calculated from the experimentally measurable quantities of pressure, temperature, specific volume, SOS, and specific heat at constant volume.

For this project, the full step-by-step derivations from three sets of foundational principles: basic thermodynamics relationships, the Maxwell and other similar relations, and properties of partial derivatives from multivariate calculus, were performed to calculate enthalpy and entropy from the measured properties in the experimental data. The enthalpy calculations are shown in Table 6 and entropy calculations are shown in Table 7. All integrals and partial derivatives are in a form that can be computed numerically from the experimental data.

CONCLUSIONS

In order to better understand the applicability of standard commercially available EOS in pipeline and compression applications, physical and thermodynamic properties of seven (7) gas mixtures representing a wide range of interest were experimentally measured under controlled conditions. These mixtures include sweet and sour natural gas and CO2 mixtures at typical pipeline and compressor conditions. The results of these measurements were then compared to the results of five EOS models for the same conditions and compositions including the GERG, NIST, AGA8, P-R, and SRK EOS. It should be noted that the predictions for a particular EOS depend on the implementation of that EOS in a particular software. The predicted results from one EOS can vary depending on the software used.

Overall, the EOS differ from each other the most near the critical point of each mixture. High concentrations of CO2 cause the largest difference between the EOS results as evident with the GMRC Mix 1, containing over 90% mol CO2. For the majority of compositions and conditions reviewed, GERG and NIST have the best correlation to measured data with AGA8 resulting in similar property predictions with few exceptions. The P-R and SRK EOS deviate the most from GERG and NIST, especially near the critical point of the mixtures for all properties and with the majority of density predictions. SRK consistently under predicts density values for all compositions and test points reviewed compared to the other EOS models. For the SOS, P-R and SRK typically over predict values across most of the compositions and conditions compared to the other EOS models. A similar over prediction trend of P-R and SRK is present in the cv EOS predictions for the majority of compositions and conditions. With the heavier hydrocarbon content of the PRCI mixtures, a shift is present in which, at lower pressures the P-R and SRK EOS provide lower values of cv than the other EOS while providing higher values at higher pressures for the majority of ranges reviewed.

Among the properties tested, the EOS model predictions provide the lowest deviation when compared to the density experimental measurement results for the compositions tested. The GERG, NIST, and AGA8 EOS fall within +/- 1% for the majority of state points in this paper, with increased deviations at elevated temperatures. The P-R and SRK EOS had higher deviations from the experimental data, under predicting density values by approximately 2% to 4% for most mixtures and conditions. When comparing the SOS measurements to the EOS results, GERG, NIST, and AGA8 do not typically deviate beyond +/- 2%. Exceptions occur near the critical point where EOS deviations increase beyond +/- 2% and with heavy hydrocarbon mixtures at lower temperatures. For the specific heat at constant volume measurements, deviations typically increase for the CO2/CH4 and sour gas mixtures as temperature increases, typically within +/- 5% from the experimental values. Deviations are at their maximum near the critical point of each mixture, specifically for the high concentration CO_2 mixture and heavy hydrocarbon mixtures. The lowest deviation from the experimental data for the compositions reviewed is the primarily methane mixture, GMRC Mix 4, with GERG, NIST, and AGA8 over predicting *cv* within 1.5%. Overall the P-R EOS had the best correlation with *cv* experimental data for GMRC Mix 2 and AGA8 provided the best results when compared to the high methane mixture, GMRC Mix 4. The highest deviations in EOS model predictions of *cv* compared to experimental values are with the PRCI defined heavy hydrocarbon mixtures. EOS deviations increased with the concentration of hydrocarbons heavier methane, with the EOS models over predicting *cv* values. Many of these deviations can be attributed to the experimental process in which the gas passes through the multiphase region. However, results still follow trends seen in other similar mixtures. Overall, the GERG, NIST, and AGA8 EOS typically provide results closer to measured values for density, SOS, and specific heat at constant volume compared to the P-R and SRK EOS based on the compositions and conditions reviewed with the exceptions noted in this paper.

In summary, it is expected that the results of this research project will help to evaluate the accuracy of existing EOS programs. However, it is also envisioned that further research is necessary.

REFERENCES

1. Botros, K., Studzinski, W., Geerligs, J., Glover, A., “Determination of Decompression Wave Speed in Rich Gas Mixtures,” Canadian Journal of Chemical Engineering, Volume 82, pp. 880-891, October 2004.

2. Kumar, S., Kurz, R, O-Connell, J, "Equations of State for Gas Compressor Design and Testing," International Gas Turbine and Aeroengine Congress & Exhibition, Indianapolis, Indiana, June 1999.
3. Magyar, R., Root, S., and Mattsson, T., "Equations of State for Mixtures, results from Density-Functional (DFT) simulations compared to High Accuracy Validation Experiments on Z," Jounral of Physics: Conference Series 500 (2014) 162004.
4. Nasrifar, K., Bollands, O., "Prediction of Thermodynamic Properties of Natural Gas Mixtures Using 10 Equations of State Including a New Cubic Two-Constant Equation of State," Journal of Petroleum Science & Engineering, 51 (2006) 253-266.
5. Sandberg, M., "Equation of State Influences on Compressor Performance Determination," Proceedings of the Thirty-Fourth Turbomachinery Symposium, 2005

Table 1. GMRC Gas Mixture Compositions

Mix	Carbon Dioxide (CO2)	Methane (CH4)	Ethane (C2H6)	Propane (C3H8)	Butane (C4H10)	Pentane (C5H12)	Nitrogen (N2)	Hydrogen Sulfide (H2S)	Water (H2O)
	% mol	% mol	% mol	% mol	% mol	% mol	% mol	% mol	% mol
1	96.8	2.3	0.3	0.08	0.02	0	0.5	0	0
2	39.6	40.79	9.9	4.95	0.79	0	2.97	0	1
3	5	46.5	8	5	3	0.5	24	8	0
4	1	95.3	2.5	0.5	0.2	0	0.5	0	0

Table 2. PRCI Gas Mixture Compositions

Mix	Carbon Dioxide (CO2)	Methane (CH4)	Ethane (C2H6)	Propane (C3H8)	i-Butane (C4H10)	n-Butane (C4H10)	i-Pentane (C5H12)	n-Pentane (C5H12)	n-Hexane (C6H14)	Nitrogen (N2)
	% mol	% mol	% mol	% mol	% mol	% mol	% mol	% mol	% mol	% mol
1	1	81.75	10	5	0.5	0.5	0.1	0.1	0.05	1
2	2	69.6	15	10	1	1	0.15	0.15	0.1	1
3	3	51.4	25	15	2	2	0.2	0.2	0.2	1

Table 3. GMRC Test Measurement Matrix

Mix	Temperature (F)	Press (psia)	Temperature (C)	Press (MPa)
1	100	300	37.78	2.07
	100	1500	37.78	10.34
	346	1500	174.44	10.34
	384	1500	195.56	10.34
	154	3500	67.78	24.13
2	100	300	37.78	2.07
	100	1500	37.78	10.34
	309	1500	153.89	10.34
	345	1500	173.89	10.34
	200	3500	93.33	24.13
	211	3500	99.44	24.13
3	120	300	48.89	2.07
	120	1500	48.89	10.34
	389	1500	198.33	10.34
	258	3500	125.56	24.13
4	100	500	37.78	3.45
	100	1500	37.78	10.34
	290	1500	143.33	10.34
	243	3500	117.22	24.13

Table 4. PRCI Test Measurement Matrix

Mix	Temp (F)	Pressure (psi)	Temperature (C)	Press (MPa)
1	32	1595.4	0	11
	122	1595.4	50	11
	212	1595.4	100	11
	32	2175.6	0	15
	122	2175.6	50	15
	212	2175.6	100	15
	32	2900.8	0	20
	122	2900.8	50	20
	212	2900.8	100	20
2	32	1595.4	0	11
	122	1595.4	50	11
	212	1595.4	100	11
	32	2175.6	0	15
	122	2175.6	50	15
	212	2175.6	100	15
	32	2900.8	0	20
	122	2900.8	50	20
	212	2900.8	100	20
3	77	1595.4	25	11
	122	1595.4	50	11
	212	1595.4	100	11
	77	2175.6	25	15
	122	2175.6	50	15
	212	2175.6	100	15
	77	2900.8	25	20
	122	2900.8	50	20
	212	2900.8	100	20

Table 5. Deviations of Predicted Physical Properties and Compressor Performance for Different Software Implementation of the SRK EOS

P1	300	300	300	300	300	300	300	300	300	301.22	301.22	**psia**
P2	1500	1500	1500	1500	1500	1500	1500	1500	1500	1499.1	1499.1	**psia**
T1	120	120	120	120	120	120	120	120	120	119.82	119.82	**Deg F**
T2	387.4	387.2	387	387	387	387	387	389.2	387	389.45	389.45	**Deg F**
Z1	0.952	0.951	0.945	0.959	0.958	0.958	0.959	0.958	0.952	0.947	0.947	
Z1 % Dev.	-0.53	-0.42	0.21	-1.27	-1.16	-1.16	-1.27	-1.16	-0.53	0.00	0.00	**%**
Z2	0.965	0.965	0.952	0.995	0.991	0.991	0.996	0.984	1	0.978	0.978	
Z1 % Dev.	1.33	1.33	2.66	-1.74	-1.33	-1.33	-1.84	-0.61	-2.25	0.00	0.00	**%**
H1				57.8	57.66	57.68	20.248					**kJ/kg**
H2				300.71	300.08	300.12	261.19					**kJ/kg**
Head	238.7	238.9	236.3	242.9	242.4	242.4	240.9	241.8		250.3	251.1	**kJ/kg**
Head % Dev	4.63	4.55	5.59	2.96	3.16	3.16	3.76	3.40		0.00	-0.32	**%**
Molecular Weight	25.826	25.826	25.826	25.825	25.825	25.825	25.825	25.825	25.819	Assumed (25.825)	Assumed (25.825)	
	RK (OEM)	***SRK (OEM)***	***SRK (OEM)***	***SRK (PVTSim)***	***SRK Peneloux (PVTSim)***	***SRK Peneloux (T) (PVTSim)***	***SRK Multi-Flash***	***SRK Refprop***	***RK (SwRI)***	***Tested (Refprop EOS Correction)***	***Tested (SRK EOS Correction)***	

Table 6. Final Results - Enthalpy

Ind. variables	Enthalpy calculation
T, P	$\Delta h_{12} = \int_{P_1}^{P_2} \left[v - T\left(\frac{\partial v}{\partial T}\right)_P \right]_{T=T1} dP + \int_{T_1}^{T_2} \left[-c_v \frac{a^2}{v^2} \left(\frac{\partial v}{\partial P}\right)_T \right]_{P=P_2} dT$
T, v	$\Delta h_{12} = \int_{T_1}^{T_2} \left[c_v + v\left(\frac{\partial P}{\partial T}\right)_v \right]_{v=v_1} dT + \int_{v_1}^{v_2} \left[T\left(\frac{\partial P}{\partial T}\right)_v + v\left(\frac{\partial P}{\partial v}\right)_T \right]_{T=T_2} dv$
P, v	$\Delta h_{12} = \int_{P_1}^{P_2} \left[c_v \left(\frac{\partial T}{\partial P}\right)_v + v \right]_{v=v_1} dP + \int_{v_1}^{v_2} \left[c_v \frac{a^2}{v^2} \left(\frac{\partial T}{\partial P}\right)_v \right]_{P=P_2} dv$

Table 7. Final Results - Entropy

Ind. variables	Entropy calculation
T, P	$\Delta s_{12} = \int_{P_1}^{P_2} \left[-\left(\frac{\partial v}{\partial T}\right)_P \right]_{T=T1} dP + \int_{T_1}^{T_2} \left[-\frac{c_v}{T}\frac{a^2}{v^2}\left(\frac{\partial v}{\partial P}\right)_T \right]_{P=P_2} dT$
T, v	$\Delta s_{12} = \int_{T_1}^{T_2} \left[\frac{c_v}{T}\right]_{v=v_1} dT + \int_{v_1}^{v_2} \left[\left(\frac{\partial P}{\partial T}\right)_v\right]_{T=T_2} dv$
P, v	$\Delta s_{12} = \int_{P_1}^{P_2} \left[\frac{c_v}{T}\left(\frac{\partial T}{\partial P}\right)_v\right]_{v=v_1} dP + \int_{v_1}^{v_2} \left[\frac{c_v}{T}\frac{a^2}{v^2}\left(\frac{\partial T}{\partial P}\right)_v\right]_{P=P_2} dv$

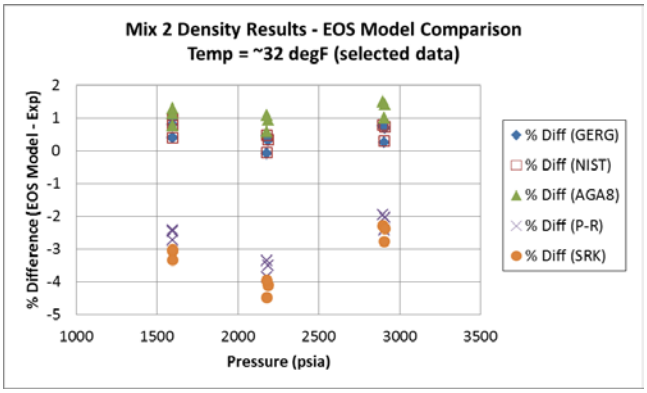

Figure 1. EOS Model Comparison with Experimental Density Data for GMRC Mix 2

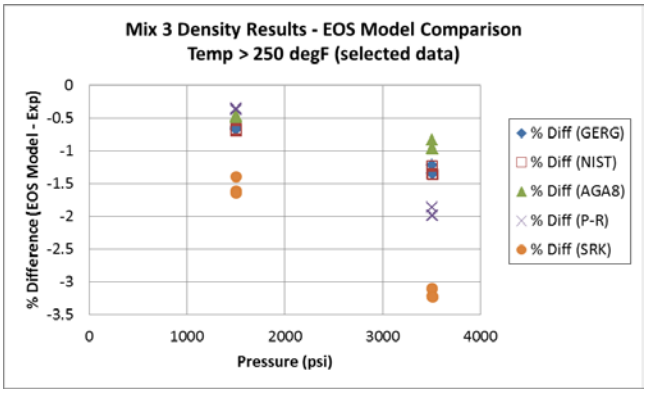

Figure 2. EOS Model Comparison with Experimental Density Data for GMRC Mix 3

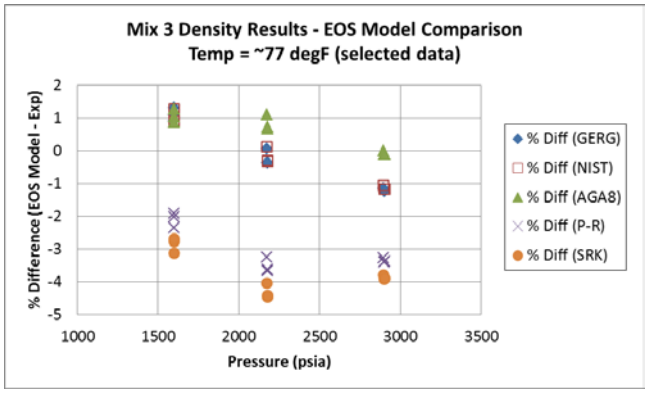

Figure 3. EOS Model Comparison with Experimental Density Data for PRCI Mix 3

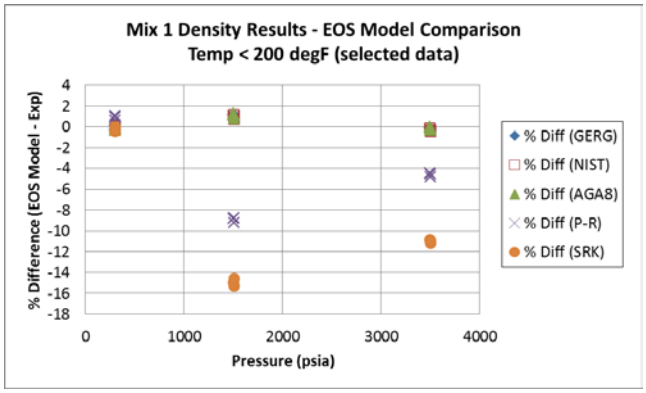

Figure 4. EOS Model Comparison with Experimental Density Data for GMRC Mix 1

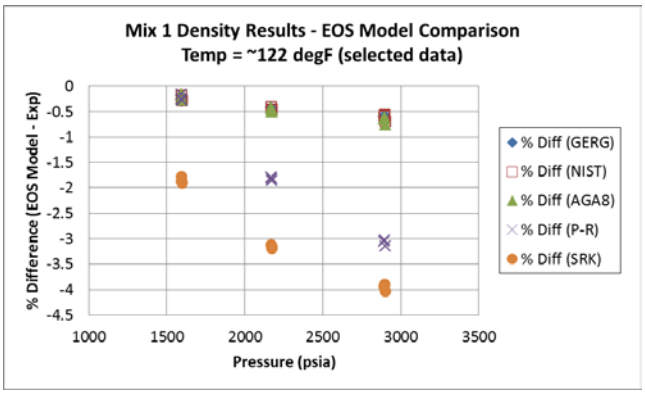

Figure 5. EOS Model Comparison with Experimental Density Data for PRCI Mix 1

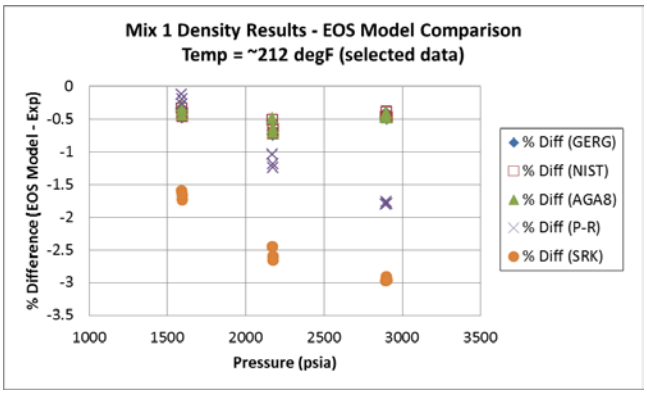

Figure 6. EOS Model Comparison with Experimental Density Data for PRCI Mix 1

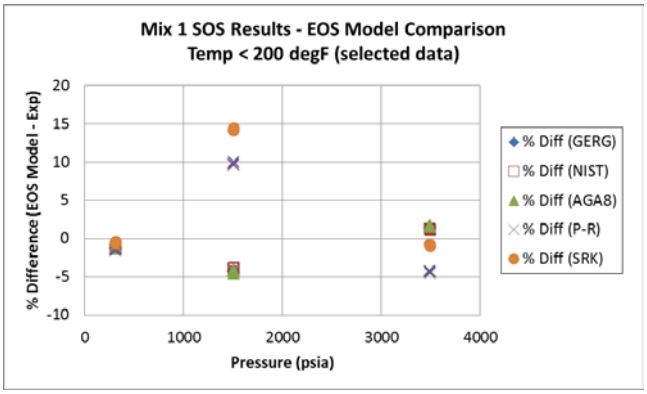

Figure 7. EOS Model Comparison with Experimental SOS Data for GMRC Mix 1

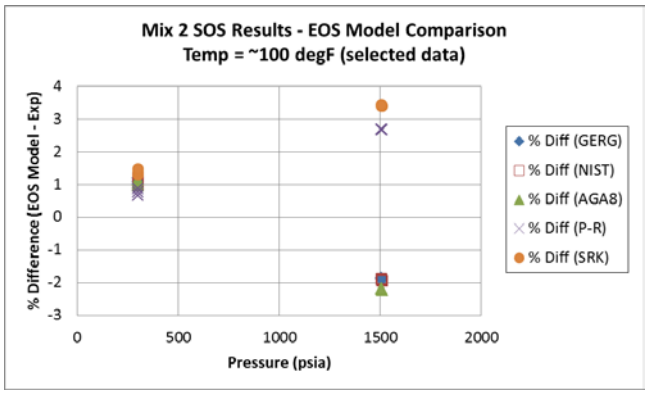

Figure 8. EOS Model Comparison with Experimental SOS Data for GMRC Mix 2

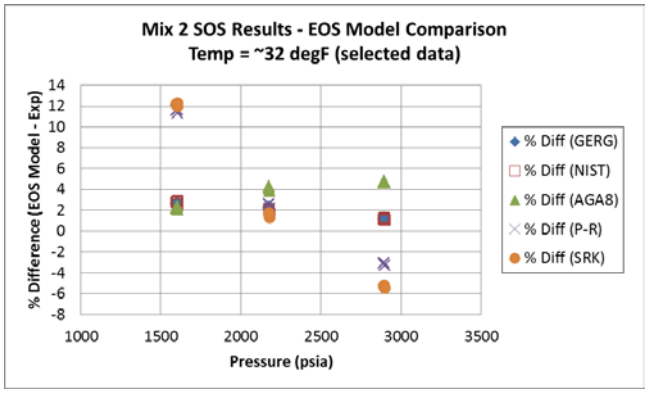

Figure 9. EOS Model Comparison with Experimental SOS Data for PRCI Mix 2

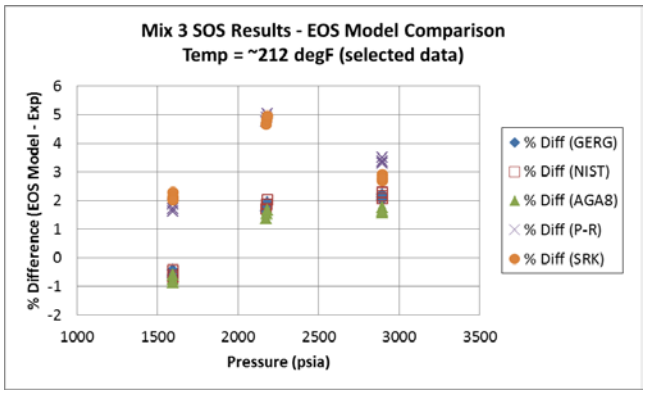

Figure 10. EOS Model Comparison with Experimental SOS Data for PRCI Mix 3

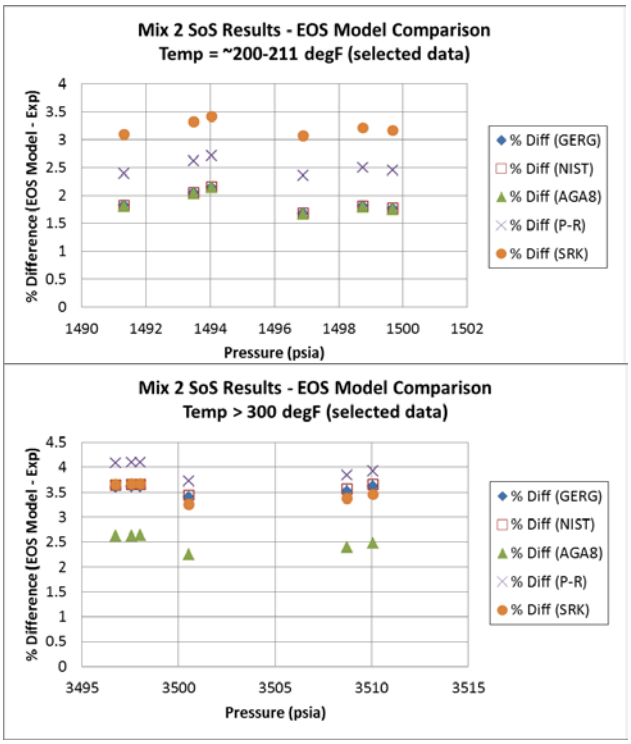

Figure 11. EOS Model Comparison with Experimental SOS Data for GMRC Mix 2

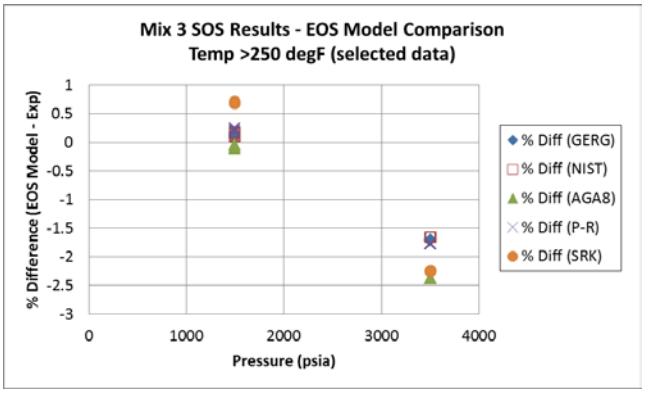

Figure 12. EOS Model Comparison with Experimental SOS Data for PRCI Mix 3

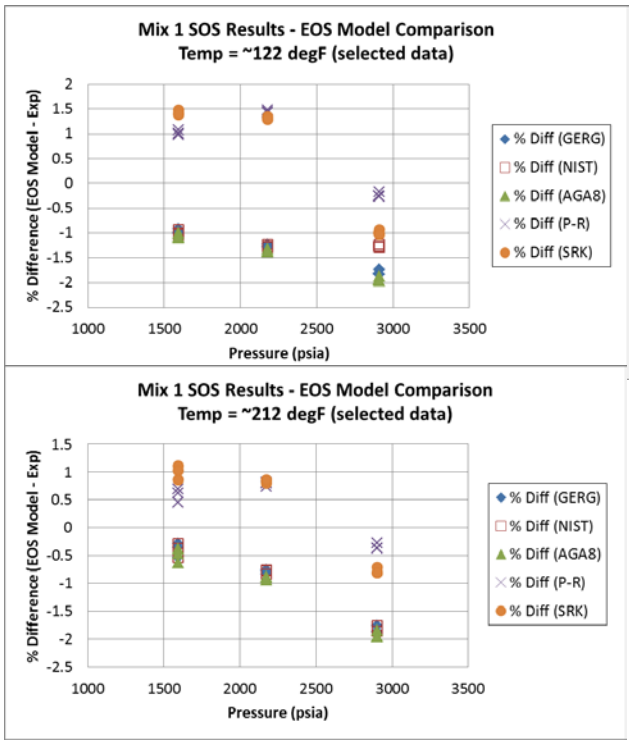

Figure 13. EOS Model Comparison with Experimental SOS Data for PRCI Mix 1

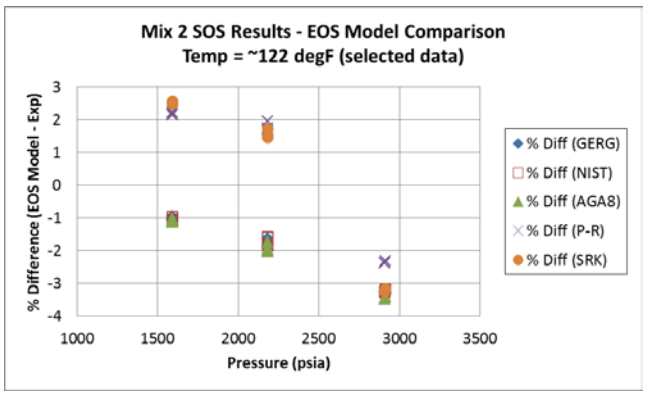

Figure 14. EOS Model Comparison with Experimental SOS Data for PRCI Mix 2

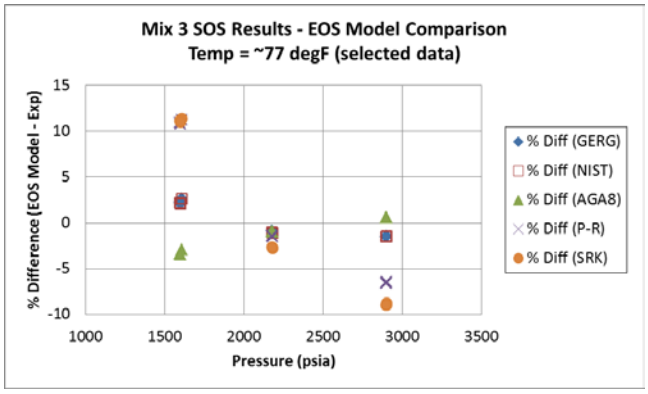

Figure 15. EOS Model Comparison with Experimental SOS Data for PRCI Mix 3

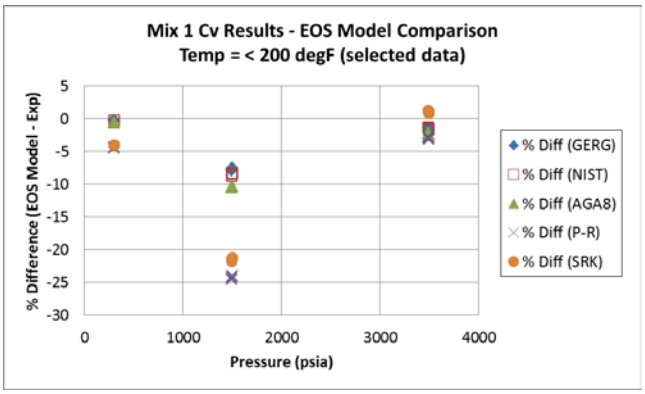

Figure 16. EOS Model Comparison with Experimental Specific Heat Data for GMRC Mix 1

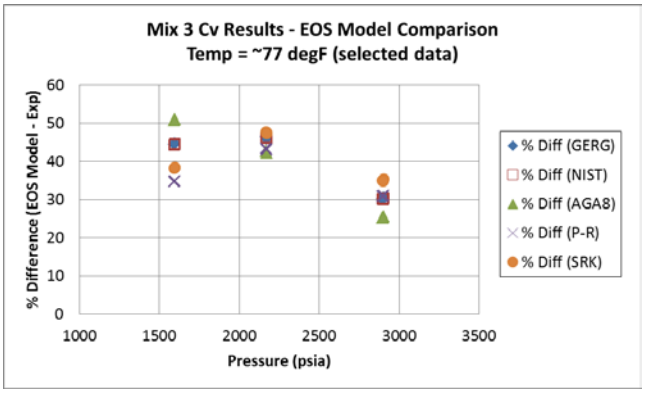

Figure 17. EOS Model Comparison with Experimental Specific Heat Data for PRCI Mix 3

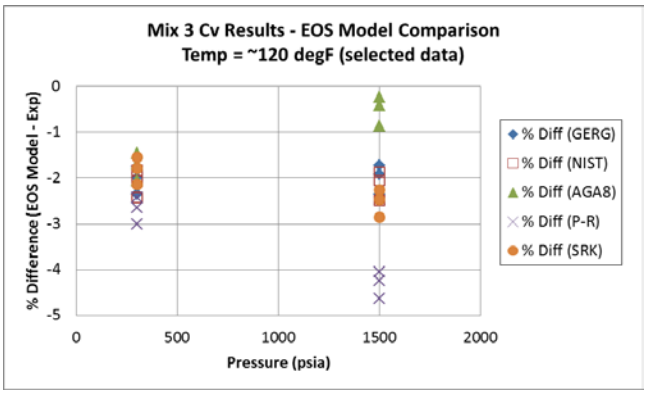

Figure 18. EOS Model Comparison with Experimental Specific Heat Data for GMRC Mix 3

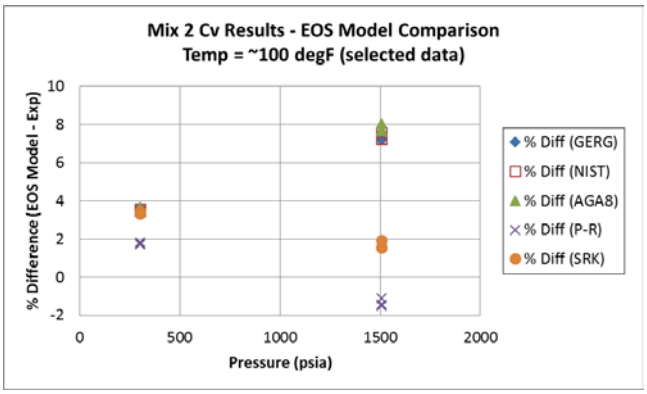

Figure 19. EOS Model Comparison with Experimental Specific Heat Data for GMRC Mix 2

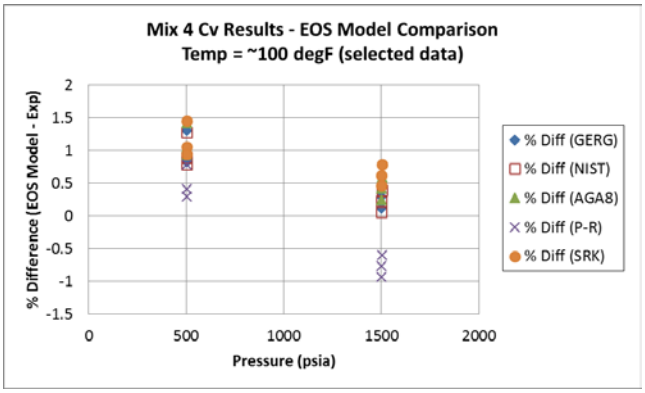

Figure 20. EOS Model Comparison with Experimental Specific Heat Data for GMRC Mix 4

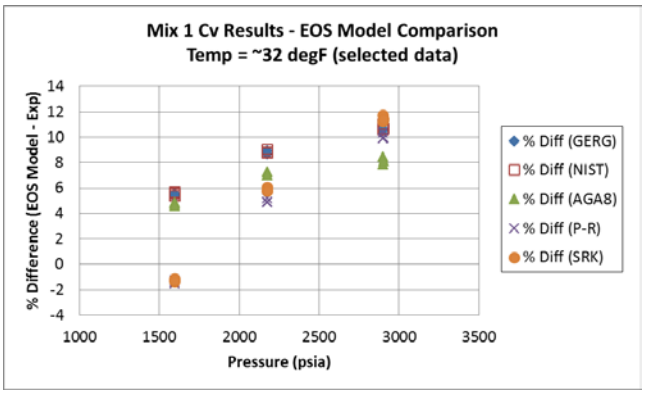

Figure 21. EOS Model Comparison with Experimental Specific Heat Data for PRCI Mix 1

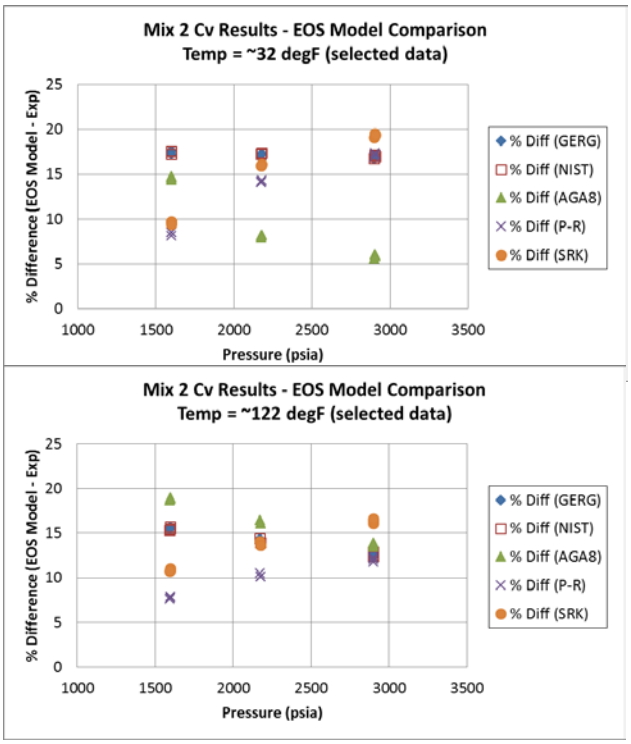

Figure 22. EOS Model Comparison with Experimental Specific Heat Data for PRCI Mix 2

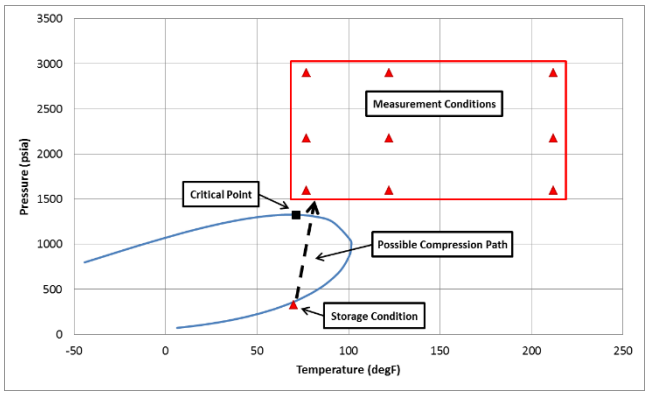

Figure 23. Phase Envelope and Critical Point as Calculated with the NIST EOS and Storage and Measurement Conditions of PRCI Mix 3

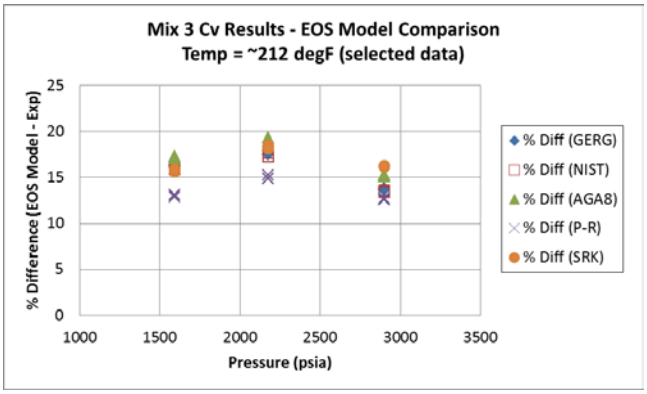

Figure 24. EOS Model Comparison with Experimental Specific Heat Data for PRCI Mix 3

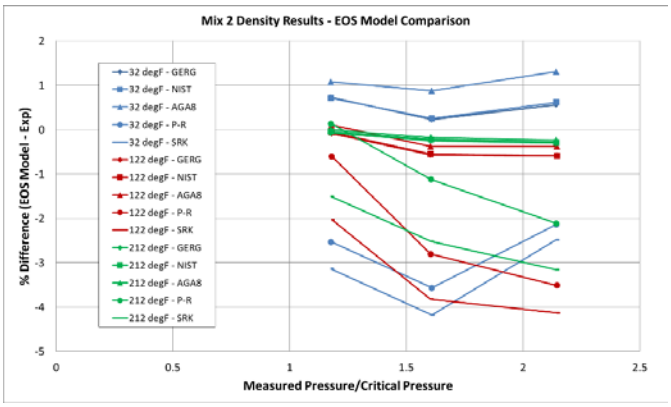

Figure 25. PRCI Mix 2 Density EOS Comparisons in Relation to Critical Point

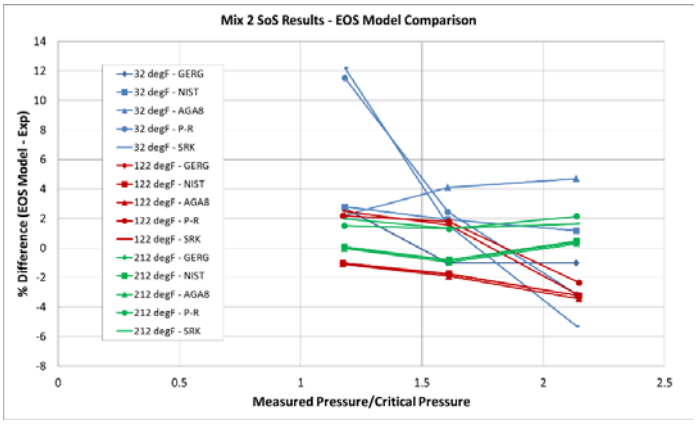

Figure 26. PRCI Mix 2 SOS EOS Comparisons in Relation to Critical Point

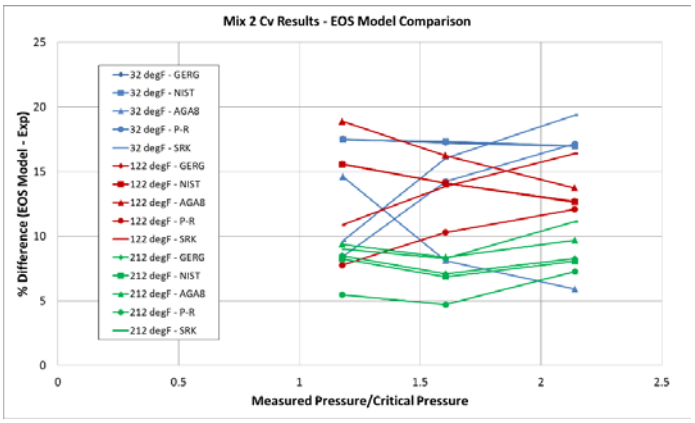

Figure 27. PRCI Mix 2 c_v EOS Comparisons in Relation to Critical Point